Variable Scale Iterative SAR Imaging Algorithm Based on Sparse Representation

Zhenzhu Zha, Qun Wan(✉), Yue Yang, Di Zhang, and Yuanyuan Song

University of Electronic Science and Technology of China, Chengdu 611731, China
wanqun@uestc.edu.cn

Abstract. In this paper, we discuss the problem of sparse recovery in compressed sensing (CS) in the presence of measurement noise, and present a variable iterative synthetic aperture radar (SAR) imaging method based on sparse representation. In this paper, the sparse reconstruction theory is applied to SAR imaging. The SAR imaging problem is equivalent to solving the sparse solution of the underdetermined equation, and the imaging result of the target scene is obtained. Compared with the previous algorithms using l_1-norm or l_2-norm as cost function model, this paper combines l_p-norm $(0<p<1)$ and l_2-norm as cost function model to obtain more powerful performance. In addition, a smoothing strategy has been adopted to obtain the convergence method under the non-convex case of l_p-norm term. In the framework of this iterative algorithm, the proposed algorithm is compared with some traditional imaging algorithms through simulation experiments. Finally, the simulation results show that the proposed algorithm improves the SAR signal recovery performance to a certain extent and has a certain anti-noise ability. In addition, the improvement is more evident when the SAR signal is block sparse.

Keywords: Synthetic aperture radar (SAR) · Sparse representation · Regularization · Block sparse

1 Introduction

SAR has recently become and will continue to be an important sensor for various remote sensing applications, especially because it overcomes some limitations of other sensing modalities. Firstly, SAR is an active sensor using its own illumination. In order to illuminate the interesting ground area, SAR sensors use microwave signals to ensure the SAR imaging capability in harsh weather conditions for 24 h without interruption. Because of these characteristics of SAR, SAR image formation has become an important research topic. The problem of SAR image formation is a typical example of the inverse problems in imaging [1].

Traditional SAR imaging synthesizes virtual antenna aperture through platform motion, achieves high resolution in azimuth direction, and achieves high resolution in range direction by pulse compression. Traditional imaging algorithms are limited by Nyquist sampling theorem in echo data sampling, which requires not only high

G. Gui and L. Yun (Eds.): ADHIP 2019, LNICST 302, pp. 219–228, 2019.
https://doi.org/10.1007/978-3-030-36405-2_23

sampling rate, but also equal interval. The transmission, storage and calculation of a large amount of data exert a great pressure on radar system, which greatly affects the real-time performance of the whole system. For example, although the Fourier transform-based PFA [1] imaging method is simple to implement and widely used, the imaging effect will inevitably be affected by side lobes, which will reduce the resolution. For the case of partial missing of the radar sampling data, the traditional PFA method often estimates missing information by linear prediction. However, the data extrapolation inevitably causes errors, so it can not get ideal imaging effect. The SAR imaging method based on sparse representation not only does not have side lobes, but also does not require uniform sampling of the observed data. It can also achieve imaging in the case of missing part of the sampled data. On the other hand, in the fields of radar imaging, communication signal and image processing, the collected observation signal is not always the final required signal, but also has to undergo some preprocessing, which obviously brings a waste of computation to signal processing. CS [2, 3] theory breaks the limitation of Nyquist theorem and is quickly applied in SAR imaging. CS theory points out that sparse signals or signals transformed into sparse signals on a set of sparse bases can be sampled at a rate much lower than the Nyquist sampling rate, and the low-dimensional signals can be recovered by some algorithms with great probability.

In 2007, Baraniuk and others first formally introduced CS theory into radar imaging [4]. For sparse scenes, under the condition of reducing the amount of sampled radar echo data, the sparse optimization algorithm can achieve high resolution non-ambiguous imaging. And the feasibility of CS in radar imaging is proved by theoretical analysis and numerical simulation experiments. In 2009, Herman et al. proposed the concept of high resolution compressed sensing radar [5, 6]. The compressed sensing radar transmits Alltop sequence signals to ensure the incoherence between transmitted signals, and then uses CS technology to reconstruct sparse scenes. In 2010, Patel et al. introduced the concept of random pulse repetition frequency into compressed sensing radar for spotlight SAR imaging. Compared with the traditional fixed pulse repetition frequency radar, the new radar system can effectively reduce the amount of echo sampling data [7]. Scholars have also studied the algorithms of sparse signal processing in typical applications such as bi-base radar imaging and multi-base radar imaging [8, 9]. With the deepening of research, sparse signal processing theory has been proved to be successful in solving the inverse problems in many applications, such as magneto-optics [10], direction of arrival estimation [11], SAR feature extraction [12], etc., and even gradually formed a sparse microwave imaging theory in the application of radar imaging. Sparse restoration methods can be classified as follows: greedy algorithms, such as Orthogonal Matching Pursuit (OMP) and Compressive Sampling Matching Pursuit (CoSaMP); probabilistic algorithms considering prior distribution of signals; convex optimization methods for solving convex relaxation problems [13].

SAR imaging based on sparse representation not only has low sampling rate, but also does not require uniform sampling, which avoids the impact of partial missing of sampling data on the imaging effect [1]. SAR imaging under sparse representation is a typical inverse problem and a typical ill-posed problem. The ill-posed problem often has no unique solution, and may even be insoluble, especially for SAR imaging under sparse representation. Sparse representation theory points out that the sampling rate

needed to recover the signal can be much smaller than that of Nyquist, so SAR imaging under sparse representation is an underdetermined set of equations. In this paper, a variable scale method using DFP formula based on sparse representation is used to solve SAR imaging problem by introducing a l_p-norm regularized sparse constraint. Article shows the performance of encouraging sparsity of the l_p-norm [14].

In the second section, we give the description of SAR echo model, and give the sparse representation form of the SAR signal. In the third section, we will introduce the proposed imaging algorithm in detail. The fourth section contains the simulation results. Finally, the conclusion is drawn in the fifth section.

2 SAR Observation Model

The SAR beam geometry and the ground plane geometry used in this paper are shown in Fig. 1. We assume that the target body coordinate system has $x - y$ (representing range and cross-range coordinates respectively), and the center of which is O in space. The coordinate system centers on the ground patch through a relatively narrow RF beam from the mobile radar. Due to the geometric structure of radar and the physical characteristics of observation process, the scattering function is included in the set of received signals. SAR continuously transmits/receives pulses to the target scene during flight. The received data are complex values, whose amplitude corresponds to the scattering signal intensity of the target, and the phase represents the scattering

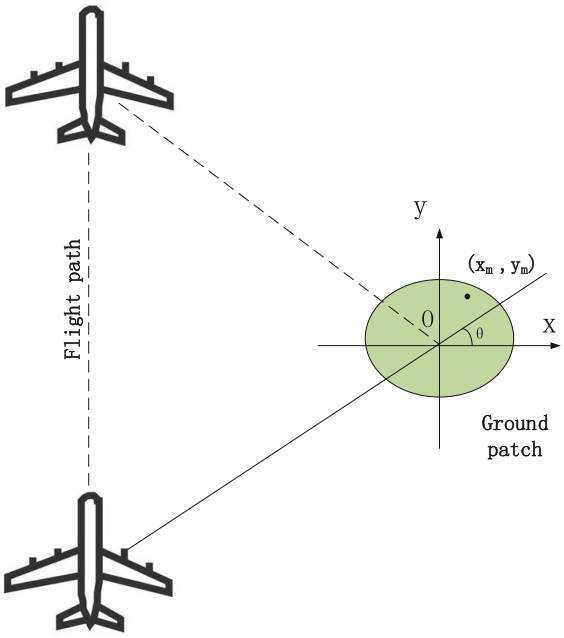

Fig. 1. Geometric model of SAR observations

characteristics. Using the high frequency hypothesis, the complex response of the target scene can be approximated to the superposition of the response of L independent scatterers in the scene. Therefore, the phase history is described as:

$$s(k,\theta) = \sum_{m=1}^{L} r(x_m, y_m) exp\{-j2k(x_m \cos\theta + y_m \sin\theta)\} \tag{1}$$

where $k = 2\pi/\lambda_0$ is the spatial frequency, θ is the azimuth, $r(x_m, y_m)$ is the scattering center coefficient at (x_m, y_m). Considering the noise environment, formula (1) can be expressed in matrix form:

$$\mathbf{s} = \mathbf{\Phi r} + \mathbf{n} \tag{2}$$

where $\mathbf{s} \in \mathbb{C}^M$ represents the measurement with noise, M is the sum of discrete sampling points of azimuth and frequency, $\mathbf{r} \in \mathbb{C}^N$ represents the SAR complex image to be reconstructed, and N is the size of the original scene, that is, the sum of discrete points of range and cross-range. $\mathbf{\Phi} \in \mathbb{C}^{M \times N}$ is the overcomplete dictionary, and $\mathbf{n} \in \mathbb{C}^M$ accounts for additive i.i.d. complex Gaussian noise.

For solving this set of equations, we need to consider the following problems: firstly, under the influence of observation noise, the system is often unsolvable, so it can not be solved directly. Secondly, if the zero space of the overcomplete dictionary $\mathbf{\Phi}$ is not empty, that is, the number of equations is less than the number of unknowns, then the solution of the set of equations is not unique. Thirdly, when the observation data $\mathbf{s}$ contains perturbations, the estimation of the target scenario $\hat{\mathbf{r}}$ remains unchanged, that is, the solution of the equation set is stable. Fourthly, the solution of the equation set should contain prior information, which conforms to the characteristics of the target scenario.

We introduce the idea of the least square to find the best matching least square solution:

$$\hat{\mathbf{r}}_{ls} = \arg\min_{\mathbf{r}} \|\mathbf{s} - \mathbf{\Phi r}\|_2^2 \tag{3}$$

But the least square solution can not guarantee the stability of the solution.

This paper assumes that the number of measurements is less than the total number of atoms in the dictionary, that is $M \ll N$. SAR imaging can be recast as a robust sparse signal recovery problem:

$$\min_{\mathbf{r}} \|\mathbf{s} - \mathbf{\Phi r}\|_0 \tag{4}$$

However, it is NP-hard to find the most sparse solution of general underdetermined equations, so the sparse constraints can be relaxed to l_p-norm $(0 < p < 1)$. Then, (4) can be expressed as a non-quadratic regularization problem:

$$\min_{\mathbf{r}} \|\mathbf{s} - \mathbf{\Phi}\mathbf{r}\|_2^2 + \mu\|\mathbf{r}\|_p \tag{5}$$

where μ is a given regularization parameter.

3 SAR Imaging Algorithm

For formula (5), we have a cost function as follows:

$$\mathbf{J}(\mathbf{r}) = \|\mathbf{s} - \mathbf{\Phi}\mathbf{r}\|_2^2 + \mu\|\mathbf{r}\|_p \tag{6}$$

To avoid the problem caused by the nondifferentiability of l_p-norm at the origin, the smoothing approximation [15] is used as follows:

$$\|\mathbf{r}\|_p \approx \sum_{i=1}^{N} (r_i^2 + \xi)^{p/2} \tag{7}$$

where ξ is a nonnegative small constant.

Therefore, the derivation of formula (6) is as follows:

$$\nabla\mathbf{J}(\mathbf{r}) = \left[2\mathbf{\Phi}^H\mathbf{\Phi} + \mu\frac{p}{2}\mathbf{D}(\mathbf{r})\right]\mathbf{r} - 2\mathbf{\Phi}^H\mathbf{s} \tag{8}$$

where H represents the conjugate transposition of the matrix and

$$\mathbf{D}(\mathbf{r}) = \begin{bmatrix} (r_1^2 + \xi)^{p/2-1} & 0 & 0 & 0 \\ 0 & (r_2^2 + \xi)^{p/2} & \cdots & 0 \\ \vdots & \vdots & \ddots & \vdots \\ 0 & 0 & \cdots & (r_N^2 + \xi)^{p/2} \end{bmatrix}$$

In this paper, a variable scale iterative method using DFP formula is considered to solve the problem. This method defines the correction matrix as follows [16]:

$$\Delta\mathbf{H}_j = \frac{p^{(j)}p^{(j)T}}{p^{(j)T}q^{(j)}} - \frac{\mathbf{H}_j q^{(j)}q^{(j)T}}{q^{(j)T}\mathbf{H}_j q^{(j)}} \tag{9}$$

Therefore, we can obtain the iterative formula:

$$\mathbf{H}_{j+1} = \mathbf{H}_j + \frac{p^{(j)}p^{(j)T}}{p^{(j)T}q^{(j)}} - \frac{\mathbf{H}_j q^{(j)}q^{(j)T}}{q^{(j)T}\mathbf{H}_j q^{(j)}} \tag{10}$$

This method does not need to compute the inverse of Hessian matrix. For general cases, the variable scale algorithm has superliner convergence rate. The implementation steps of sparse variable scale iterative (SVSI) SAR imaging algorithm are shown at Table 1.

Table 1. The implementation steps of SVSI SAR imaging algorithm

	SVSI algorithm
1.	Initialize $\mathbf{r}^{(1)}$, $\mathbf{H}_1 = \mathbf{I}_N$.
2.	Let $j = 1$ and calculate the gradient at $\mathbf{r}^{(1)}$: $$\mathbf{g}_1 = \nabla \mathbf{J}(\mathbf{r}^{(1)}).$$
3.	Let $\mathbf{d}^{(j)} = -\mathbf{H}_j \mathbf{g}_j$.
4.	Starting from $\mathbf{r}^{(j)}$ and searching along direction $d^{(j)}$, the step size λ_j is obtained to satisfy the requirement: $$\mathbf{J}(\mathbf{r}^{(j)} + \lambda_j \mathbf{d}^{(j)}) = \min_{\lambda \geq 0} \mathbf{J}(\mathbf{r}^{(j)} + \lambda \mathbf{d}^{(j)})$$ then let $\mathbf{r}^{(j+1)} = \mathbf{r}^{(j)} + \lambda_j \mathbf{d}^{(j)}$.
5.	Stop when $\left\|\mathbf{r}^{(j+1)} - \mathbf{r}^{(j)}\right\| \Big/ \left\|\hat{\mathbf{r}}^{(j)}\right\|$ is less than a predetermined threshold ε. Let $\hat{\mathbf{r}} = \mathbf{r}^{(j+1)}$. Otherwise, turn to step 6.
6.	If $j = N$, let $\mathbf{r}^{(1)} = \mathbf{r}^{(j+1)}$, and return to step 2. Otherwise proceed to step 7.
7.	Let $\mathbf{g}_{j+1} = \nabla \mathbf{J}(\mathbf{r}^{(j+1)})$, $\mathbf{p}^{(j)} = \mathbf{r}^{(j+1)} - \mathbf{r}^{(j)}$, $\mathbf{q}^{(j)} = \mathbf{g}_{j+1} - \mathbf{g}_j$. Set $j := j + 1$.

4 Simulation Experiment

The convergence speed of SVSI is related to the initial value. If the initial value close to the real value can be used, the computation will be greatly reduced. In this paper, $\hat{\mathbf{r}}^{(1)} = 2\kappa \mathbf{\Phi}^H \mathbf{s}$ is used as the initial input and the convergence speed is faster. In this section, the effectiveness of the proposed method is demonstrated by combining the simulation experiment of a group of radar observations. The radar parameters used in the experiment are shown at Table 2. This paper defines the normalized mean squared error NMSE = $\|\hat{\mathbf{r}} - \mathbf{r}\|_2^2 \Big/ \|\mathbf{r}\|_2^2$ as the evaluation index. The smaller the NMSE, the higher the image reconstruction quality. Next, we give the experimental results to verify the application effect of SVSI algorithm in sparse SAR imaging and block sparse SAR imaging.

Table 2. SAR system parameters.

SAR system parameters	
Bandwidth (MHz)	800
Center frequency (GHz)	9
The observation azimuth	87.5°–92.5°
Frequency sampling points	23
Azimuth sampling points	23
The signal-to noise ratio (SNR/dB)	30

Figure 2 shows the comparison of reconstructed images with different SNR. (a) and (b) are the original scene and the recovery result of PFA, respectively. (c) and (e) are the recovery results of LS algorithm and SVSI algorithm with SNR = 5 dB, and (d) and (f) with SNR = 20 dB. From Fig. 2, we can see that the traditional PFA is the worst, and the LS algorithm is more depend on the high SNR. And the proposed algorithm stably behaves good performance. In the Fig. 3, we apply the SVSI algorithm to block sparse SAR data, and the results show that when the sampling data becomes bigger and the inner structure of data is more complex, the PFA algorithm and LS algorithm are failed to reconstruct SAR image. However, SVSI algorithm reasonably reconstructs SAR image with a low NMSE = 0.0011. So we can see the improvement of the performance of the proposed algorithm and its possibility of application in the reconstruction of the block sparse SAR.

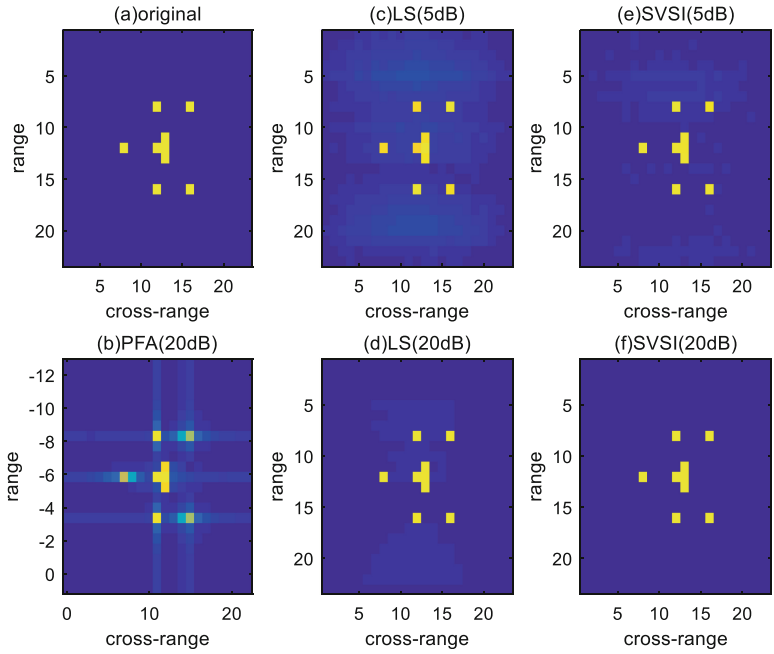

Fig. 2. The comparison of reconstructed images with different SNR. (a) the original scene. (b) the result of PFA with SNR = 20 dB. (c) the result of LS with SNR = 5 dB. (d) the result of LS with SNR = 20 dB. (e) the result of SVSI with SNR = 5 dB. (c) the result of SVSI with SNR = 20 dB.

Figure 4 shows the NMSE comparison of the least square algorithm and the SVSI algorithm with the variable SNR. SNR range from 5 dB to 40 dB. And form Fig. 4, we can see that with the increasing of SNR, that is to say the additive complex Gaussian noise is decreasing, NMSE both of LS and SVSI are decreasing. In addition, when SNR is relatively low, the performance of LS is so bed that sometimes it even can't to

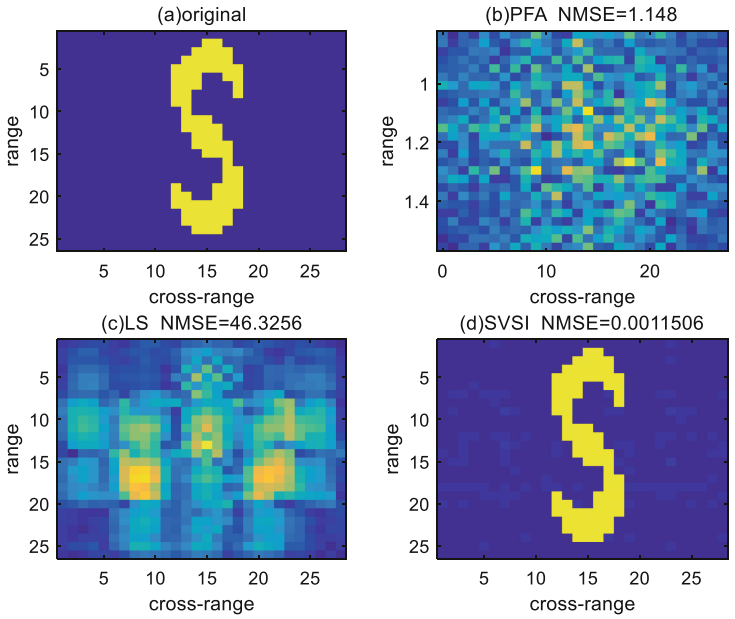

Fig. 3. The proposed algorithm is applied to block sparse SAR signal (SNR = 30 dB). (b) NMSE of PFA is 1.148. (c) NMSE of LS is 46.326. (d) NMSE of SVSI is 0.0011.

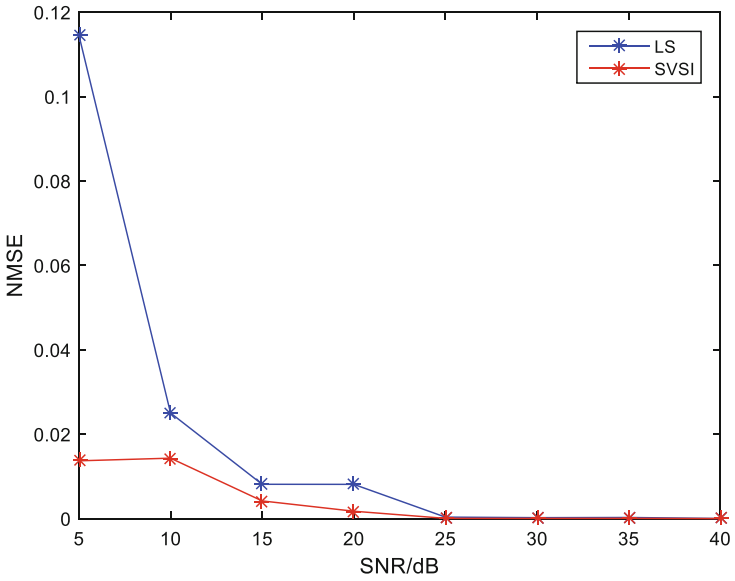

Fig. 4. The NMSE comparison of the least square algorithm and the SVSI algorithm with the variable SNR. SNR range from 5 dB to 40 dB.

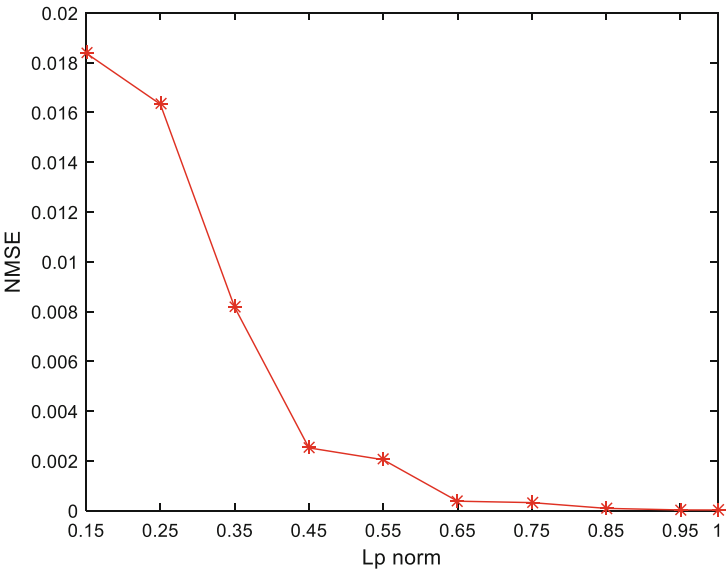

Fig. 5. The SVSI algorithm: the curve of NMSE with different value p.

reconstruct image. This result also illustrates that the proposed algorithm has a certain anti-noise ability. Figure 5 is the curve of NMSE with different l_p-norm. And SNR is 30 dB. From the curve, we know that the value of p is not randomly determined. When it's too small, the result becomes a little awful. So we should take an appropriate value.

5 Conclusion

This paper presents a SAR imaging algorithm based on sparse representation, which has the following advantages: no need to calculate the Hessian matrix; having a super-linear convergence rate. However, when the amount of data becomes large, the amount of storage required will become a problem. In the SAR synthesis scenario of this paper, it can be seen from the simulation results that the proposed algorithm not only performs well in sparse SAR image reconstruction, but also maintains good performance in the case of block sparse SAR. And at low SNR, it can also reconstruct SAR images completely with a tolerable NMSE, showing a certain anti-noise ability.

Acknowledgments. The authors would like to thank the anonymous reviewers for their careful review and constructive comments. This work was supported in part by the National Natural Science Foundation of China (NSFC) under Grant 61771108 and U1533125, and the Fundamental Research Funds for the Central Universities under Grant ZYGX2015Z011.

References

1. Li, X.: Synthetic aperture radar image formation for distributed target with sparse representation, pp. 12–28 (2016)
2. Donoho, D.L.: Compressed sensing. IEEE Trans. Inf. Theory **52**(4), 1289–1306 (2006)
3. Candes, E.J., Wakin, M.: An introduction to compressive sampling. IEEE Signal Process. Mag. **25**(2), 21–30 (2008)
4. Baraniuk, R., Steeghs, P.: Compressive radar imaging. In: IEEE Radar Conference, Boston, pp. 128–133 (2007)
5. Herman, M., Strohmer, T.: Compressed sensing radar. In: Proceedings in IEEE Radar Conference, Rome, pp. 1–6 (2008)
6. Herman, M., Strohmer, T.: High-resolution radar via compressed sensing. IEEE Trans. Signal Process. **57**(6), 2275–2284 (2009)
7. Patel, V.M., Easley, G.R., Healy, D.M.: Compressed synthetic aperture radar. IEEE J. Sel. Top. Signal Process. **4**(2), 244–254 (2010)
8. Stojanovic, I., Karl, W.C.: Imaging of moving targets with multi-static SAR using an overcomplete dictionary. IEEE J. Sel. Top. Signal Process. **4**(1), 164–176 (2010)
9. Ludger, P.: Application of compressed sensing to SAR/GMTI-Data. In: European Conference on Synthetic Aperture Radar, Aachen, pp. 7–10 (2010)
10. Zhang, Z., Rao, B.D.: Sparse signal recovery with temporally correlated source vectors using Sparse Bayesian Learning. IEEE J. Sel. Top. Signal Process. **5**, 912–926 (2011)
11. Tzagkarakis, G., Milioris, D., Tsakalides, P.: Multiple-measurement Bayesian compressed sensing using GSM priors for DOA estimation. In: IEEE International Conference on Acoustics, Speech and Signal Processing (ICASSP), Dallas, pp. 2610–2613 (2010)
12. Cong, X.C., Zhu, R.Q., Liu, Y.L.: Feature extraction of SAR target in clutter based on peak region segmentation and regularized orthogonal matching pursuit. In: Signal and Information Processing (ChinaSIP), pp. 189–193 (2014)
13. Elad, M.: Sparse and Redundant Representations: From Theory to Applications in Signal and Image Processing. Springer, New York (2010). https://doi.org/10.1007/978-1-4419-7011-4
14. Wen, F., Liu, P., Liu, Y.: Robust sparse recovery in impulsive noise via $l_p - l_1$ optimization. IEEE Trans. Signal Process. **65**(1), 105–118 (2017)
15. Özben Önhon, N.: A sparsity-driven approach for joint SAR imaging and phase error correction. IEEE Trans. Image Process. **21**(4), 2075–2088 (2012)
16. Baolin, C.: Optimization Theory and Algorithm, 2nd edn. Tsinghua University Press, Beijing (2005)